# Normal faults and thrusts re-activated by deep fluids: the 6 April 2009 Mw 6.3 L'Aquila earthquake, central Italy.

Di Luccio[1], F., Ventura[1] G., Di Giovambattista[2] R., Piscini[2] A., Cinti[1] F. R.,

[1] Istituto Nazionale di Geofisica e Vulcanologia, Sismologia e Tettonofisica, Via di Vigna Murata 605, 00143 Roma, Italy.
[2] Istituto Nazionale di Geofisica e Vulcanologia, Centro Nazionale Terremoti, Via di Vigna Murata 605, 00143 Roma, Italy.

Corresponding author: Francesca Di Luccio, Istituto Nazionale di Geofisica e Vulcanologia, Sismologia e Tettonofisica, Via di Vigna Murata 605, 00143 Roma, Italy. Phone (+39) 06-51860561 , Fax (+39) 06 51860507 e-mail: francesca.diluccio@ingv.it

**Abstract**

On April 6 2009, a $M_w$=6.3 earthquake occurred in the central Apennines (Italy) damaging L'Aquila city and the surrounding country. We relocate the October 2008-April 6 2009 foreshocks and about 2000 aftershocks occurred between April 6 and April 30 2009, by applying a double-difference technique and determine the stress field from focal mechanisms. The events concentrate in the upper 15 km of the crust. Three main NW-SE to NNW-SSE striking, 30°-45° and 80°-90° dipping faults activate during the seismic sequence. Among these, a normal fault and a thrust were re-activated with dip-slip movements in response to NE-SW extension. The structural maturity of the seismogenic fault system is lower than that displayed by other systems in southern Apennines, because of the lower strain rate of the central sector of the chain with respect to the southern one. $V_P/V_S$ increases progressively from October 2008 to the April 6 2009 mainshock occurrence along a NW-SE strike due to an increment in pore fluid pressure along the fault planes. Pore pressure diffusion controls the space-time evolution of aftershocks. A hydraulic diffusivity of 80 $m^2/s$ and a seismogenic permeability of about $10^{-12}$ $m^2$ suggest the involvement of gas-rich ($CO_2$) fluids within a highly fractured medium. Suprahydrostatic, high fluid pressure (about 200 MPa at 10 km of depth) within overpressurized traps, bounded by pre-existing structural and/or lithological discontinuities at the lower-upper crust boundary, are required to activate the April 2009 sequence. Traps are the storage zone of $CO_2$-rich fluids uprising from the underlying, about 20 km deep, metasomatized mantle wedge. These traps easily occur in extensional regimes like in the axial sector of Apennines, but are difficult to form in strike-slip regimes, where sub-vertical faults may cross the entire crust. In the Apennines, fluids may activate faults responsible for earthquakes up to $M_w$=5-6. Deep fluids more than tectonic stress may control the seismotectogenesis of accretionary wedges.

## 1. Introduction

On April 6 2009, a destructive (about 300 casualties), $M_w$=6.3 earthquake hits L'Aquila city and the central sector of the Apennines, Italy (Fig. 1a,b). Additional damage was produced by the two larger aftershocks located to the south (April 7, $M_w$=5.6) and north (April 9, $M_w$=5.4) of the epicentral area. The Neogene Apennines folds-and-thrust belt represents the accretionary wedge of a subduction zone that includes, to the west, the Tyrrhenian back-arc basin and, to the east, the Adriatic-Apulian foreland and foredeep (Fig. 1a) [*Malinverno and Ryan*, 1986; *Doglioni*, 1991]. At present, the central sector of the chain is affected by a NE-SW striking extension and uplift (up to 2.5-3.0 mm/yr) [*Hunstad et al.,*2003]. This extension is responsible for the formation of intra-mountain basins bounded by NW-SE striking normal faults [*Patacca et al.*, 2008]. The seismic activity of Apennines concentrates in the axial sector of the chain [http://emidius.mi.ingv.it/CPTI08/] (Fig. 1c) [*Ventura et al.*, 2007]. The geodynamic significance of such seismicity is still debated and different, not necessarily in conflict, hypotheses have been done: (a) following *Chiarabba et al.* [2005 and reference therein], the Apennines earthquakes are related to the northeastward retreat of the Adria-Ionian lithosphere; (b) according to *Patacca et al.* [2008], the seismic activity is due to the gravity adjustment of the upper crust related to an increase of the structural relief caused by an out-of-sequence propagation of active thrusts at depth; (c) *Lavecchia et al.* [2003] propose that the Apennines earthquakes reflect rifting processes associated to large-scale plume-induced lithospheric stretching in the Tyrrhenian domain; (d) following other authors, the seismicity is due to the upward and eastward migration in the crust of $CO_2$-rich fluids from a partly metasomatized mantle wedge beneath the chain axis [*Ghisetti and Vezzani*, 2002, *Chiodini et al.*, 2004; *Ventura et al.*, 2007; *Frezzotti et al.,* 2009]. The role of fluids in northern Apennines is emphasized by a recent study by *Miller et al.* [2004], which propose that aftershocks of the 1997 crustal earthquakes were driven by the coseismic release of fluids through ruptures created by the larger events.

Here, we study the $M_w^{max}$=6.3 April 2009 L'Aquila seismic sequence in the central Apennines. Previous studies [*Chiarabba et al.*, 2009] analyze the distribution of the 712 better localized events and conclude that a poorly known normal fault accommodates the extension of the area. We locate the foreshocks and about 2000 aftershocks using a double difference method, analyze the spatial distribution of the events, determine the stress field, and study the $V_p/V_s$ variations. The collected data and results are discussed in light of the available geological and geophysical information and allow us to put constraints on (a) the activation of inherited faults (e.g. pre-existing thrusts), (b) the role of deep fluids in the nucleation process, and (c) the active geodynamics in accretionary wedges.

## 2. Geological setting and seismotectonics

The Apennines chain resulted from the contemporaneous opening of the Tyrrhenian Sea, the eastward migration of a compressive front, and the retreat of the lithospheric plate dipping below the Italian peninsula (Fig. 1a) [*Malinverno and Ryan*, 1986; *Doglioni*, 1991, 1995]. Due to the eastward migration of the compressive front since the Early Miocene, back-arc extension  affected areas which were previously controlled by compressive tectonics. Evidence of these compressive tectonics is represented by NW–SE striking thrusts, which place the carbonate Meso-Cenozoic succession in contact with the Miocene arenaceous flysch. The subsequent extensional tectonics has been conditioned in many cases by the geometry of the older thrust systems, with re-activation of pre-existing structures [*Galadini and Galli*, 2000]. Since the Pliocene, NW–SE striking normal faults have been responsible for the formation of large intermountain basins in which Plio-Quaternary continental sediments deposited. While compressive structures (over-thrusts) characterize the Apennines front, normal faults affect the Apennines chain from Pleistocene time [*Doglioni*, 1995]. Data from a NE-SW striking seismic profile located 35 km south of the 2009 L'Aquila seismic sequence evidences nappes of Mesozoic-Triassic carbonates displaced by low-angle thrusts, that also involve lower Pliocene terrains (Fig. 1b,c) [*Ghisetti and Vezzani*, 2002; *Patacca et al.*, 2008; *Di Luzio et al.*, 2009]. The Upper Pliocene-Quaternary deposits and the underlying units are cut by normal faults, extending in depth to 10-15 km, with dip ≥45°. A Moho doubling under the central Apennines reflects the geometry of the mantle wedge between the subducting Adriatic lithosphere and the Apennines chain (Fig. 1c). The April 2009 L'Aquila seismic sequence occurred in the central sector of Apennines, in an area characterized by anomalous low compressional velocity ($V_P$) and low attenuation (*Q*) at depth larger than 20 km probably due to a fluid-rich zone and heating from the underlying mantle wedge (Fig. 1b) [*Mele et al.*, 1996; *Di Stefano et al.*, 1999]. According to *Chiodini et al.* [2000], the aquifers of this area are affected by a relevant, mantle- derived $CO_2$ flux with values in the order of $10^6$ mol $km^{-2}$ $yr^{-1}$ (Fig. 1b).

L'Aquila basin is bounded by the Gran Sasso and Mt. d'Ocre ranges, and by normal faults delimiting intra-mountain sub-basins (Fig. 2). The main geological units of the area can be summarized as follows. Jurassic-Miocene limestones and marls, and Miocene sandstones represent the bedrock outcropping on the ridges and valley flanks. Quaternary deposits include Pleistocene breccias and lacustrine deposits [*Blumetti et al.,* 2002]. Local debris alluvial fans occur at the foot of the valley.

On the eastern side of the Aterno river valley (Fig. 2), south-western dipping faults occur while antithetic faults affect the western side. The active faults strike (N)NW–(S)SE, and dip 45° to 70° [*Galadini and Galli*, 2000] (Fig. 2). They are characterized by normal to normal-oblique slips and move in response to a NE-SW extension, which is acting at regional scale [*Montone et al.*, 2004 and reference therein]. Pre-existing, NNE-SSW and ESE-WNW to NW-SE, low-angle (dip<45°) structures also outcrop (Fig.1b) [*Pizzi and Galadini*, 2009]. The structural arrangement of the L'Aquila area results from the superimposition of the Quaternary extensional tectonics (Early Pleistocene-to date) to the Neogene compressive one [*Ghisetti and Vezzani*, 1999].

The Late Quaternary surface faulting associated to earthquakes larger than M>5.5 mostly occurred on the NW-SE striking faults. It is noteworthy that one of the NW-SE normal faults bordering the northern side of the Aterno basin, i.e. the Paganica fault, reactivated during the April 2009 L'Aquila sequence and surface faulting was observed for a length of about 3 km [*Emergeo Working Group*, 2010].

Historical seismicity [http://emidius.mi.ingv.it/CPTI08/] indicates that the region was affected by destructive earthquakes (Fig. 2). The main events occurred in 1349 AD ($M_e$=6.5), 1461 ($M_e$=6.4), 1703 ($M_e$=6.7) and 1762 ($M_e$=6.0). *Tertulliani et al.* [2009] observe strong analogies in the intensity distribution and the areas of the strongest effects produced by the historical shocks and those occurred on April 2009. *Bagh et al.* [2007] report that the background seismicity of the area is characterized by earthquakes with $M_L \leq 3.7$ and it is locally clustered. The seismogenic volume affects the upper 15 km of the crust.

## 3. The seismic sequence and event location

### *3.1 Methods*

About 20000 aftershocks were recorded by the national seismic network of the Istituto Nazionale di Geofisica e Vulcanologia (INGV) up to September 2009. We used the P and S wave readings from the INGV bulletin and relocated the seismicity occurred within one month from the mainshock (April 6 2009) and the foreshocks from October 2008 to April 6 2009. We used HYPOINVERSE code [*Klein*, 2000] to get a first located dataset, and then applied the double-difference technique [HypoDD by *Waldhauser and Ellsworth*, 2000] to better constrain the seismicity. The HypoDD method bases on a two-step process: in the first step, the travel time differences for event pairs at common stations are derived from the analysis of the catalogue data, then in the second step the computed differential travel time data are used to calculate double-difference hypocentral locations. HypoDD technique considers only events with a number of observations greater than a fixed value and they are grouped into clusters of well-linked earthquakes (events belong to only one cluster and that are not connected to other clusters) to insure stability of the inversion. A 1D velocity model from *Bagh et al.* [2007] in the initial location as well as in the relocation procedure is used, with a Vp/Vs of 1.86. In this study, the minimum number of observations per event pair is 8 and the maximum hypocentral separation allowed between linked events was fixed at 10 km. We obtain travel time differences for each event pair with a separation distance <10 km at stations located within 60 km distance from the cluster centroid. We use P and S wave picks equally weighted from 32 seismic stations of the INGV seismic network, and, for most of the aftershocks, readings from temporary networks installed after the mainshock occurrence are also included. The INGV location of the April 6 2009 mainshock is 42.35 N, 13.38 E, and focal depth 9.46 km [http://portale.ingv.it].

We relocate more than 2000 events. Seventy-five per cent of the double-difference locations have uncertainty <300 m in horizontal direction, and 400 m is the depth resolution ($\Delta z$); for the remaining 25%, the horizontal resolution is < 400 m, while $\Delta z$ is < 600 m.

### *3.2 Results*

The obtained relocations, shown in Fig. 3, are grouped in a narrow zone both in depth and map view. Fig. 3a shows three main clusters of seismicity. The epicenter area evidences a roughly NW-SE aligned seismicity with focal depths mostly between 5 and 12 km (Fig. 3b profile 3). The northernmost cluster, which includes the $M_w$=5.4 aftershock of April 9, is NW-SE oriented. South of the April 6 mainshock, a dense area of seismicity, including the $M_w$=5.6 aftershock of April 7 is roughly NNW-SSE oriented. The focal depths are generally deeper than 6 km (Fig. 3b profile 4). It is noteworthy that the three recognized clusters are spatially well localized, and rare seismicity characterizes the inter-cluster areas. Foreshocks concentrate immediately south of the April 6 mainshock and their focal depth extend from 4 to 12 km (Fig. 3b).

The cross-sections 1, 2 and 3 in Fig. 3b are NE-SW oriented, while section 4 strikes WSW-ESE. In the profile 1, which has a width of 10 km, the seismicity depicts three sub-vertical clusters with depths reaching 12 km with the stronger aftershock at 11 km. The westernmost cluster includes the events belonging to the north-western tip of the April 6 mainshock area, whereas the other two clusters include events associated to the April 9 $M_w$=5.4 aftershock. Sparse earthquakes with depth between 12 and 18 km also occur.

The cross-section 2 (Fig. 3b) has a width of 6 km. Two dense sub-vertical clusters are identified: the westernmost one includes most of the April 6 aftershocks with depths roughly between 7 and 11 km, whereas the easternmost one is slightly shallower. Between the two clusters, earthquake distribution reveals two planes dipping about 45° and 30° towards SW.

The earthquakes on the cross-section 3 (width 10 km) in Fig. 3b depict a 45°, southwest dipping plane between 11 and 7 km of depth. The prolongation of this plane, which includes the April 6 mainshock, to the surface intercepts the trace of the Paganica fault, where alignment of continuous surface breaks is observed [*Emergeo Working Group*, 2010]. From 7 to 5 km of depth, the dip of the above described plane decreases to about 20°-30°. Finally, a minor group of few events is depicted at about 10 km of depth, 5 km away from the mainshock. The April 6 foreshocks (Fig. 3b) are between 9 and 11 km of depth, with few shallower events describing a vertical cluster and other few events located northeastward of the April 6 mainshock at about 7 km of depth.

The section 4 in Fig. 3b has a width of 4 km, and it is centered on the April 7 $M_w$=5.6 aftershock. The seismicity concentrates between 7 and 12 km in depth, with the April 7 aftershock at 14 km. As evidenced in the profile 4 (Fig. 3b), the seismicity depicts a dense cloud of events without preferred alignments.

As a consequence, the rupture plane associated to the April 7 event could be either the approximately EW oriented fault plane or the N-NW oriented plane (see focal mechanism in Fig.3a). A recent study by *Pino and Di Luccio* [2009] reveals, however, that the preferred rupture plane is the N-NW oriented, which is also consistent with the epicentral distribution of aftershocks (Fig. 3a).

## 4. Stress field

Focal mechanisms of the larger foreshocks and aftershocks of the April 2009 sequence ($M_w$>3), available on line at http://eqinfo.eas.slu.edu/Earthquake_Center/MECH.IT/, were analyzed. The focal solution of the aftershocks are consistent with normal slips (Fig. 3a). The solutions of the foreshocks indicate normal and oblique slips. Nodal planes of 35 focal mechanisms show a clear NW-SE preferred strike along planes dipping 45° toward SE (Fig. 4a,b). A minor N-S strike is also present. The preferred strike is consistent with the elongation of the April 6 2009 aftershock zone (Fig. 3a). The N-S strike is roughly compatible with the elongation of the aftershocks associated to the $M_w$=5.6 April 7 event. We use 35 focal mechanisms of significant earthquakes to compute the stress field, by applying the method developed by *Michael* [1987]. Results are reported in Fig. 4c and indicate a normal stress field characterized by a sub-horizontal, NE-SW striking minimum compressive stress $\sigma_3$. This stress configuration is consistent with that acting in the central Apennines [*Montone et al.*,2004; *Bagh et al.*, 2007].

## 5. $V_p/V_s$

Foreshocks of the April 6 mainshock started mainly from October 2008 and concentrated at about 9-11 km of depth (Fig. 3b). The cumulative number of events as a function of time prior to the mainshock clearly shows a significant increase in the total number of recorded earthquakes (Fig. 5). Three main trends of seismicity rate defined by jumps in the cumulative number of events are evident. We estimated $V_P/V_S$ from the foreshocks by applying the modified Wadati method [*Wadati*, 1933] to each of the identified three trends with constant seismic rate. The starting dataset including P and S phases with weight ranging between 0 and 4 was restricted to a subset of clear, sharp onsets most of which having 0 weight. Taking into account the real uncertainty on DTp and DTs, the obtained $V_P/V_S$ was fitted using a linear least-square regression with a correlation coefficient varying between 0.92 and 0.98 for the time periods in Fig. 5 and between 0.78 and 0.94 for the AQU-FIAM and AQU-FAGN paths in Fig. 6. The lowest value of 0.78 was obtained for the period March 2009-April 6 2009 relative to the AQU-FAGN path (Fig. 6), whose data are more sparsely distributed with respect to the other path and/or time periods. We selected the arrival times from the nearest stations distributed around the epicentral area. The Wadati plot (Fig. 5) referring to the October 2008-January 2009 period shows a $V_P/V_S$= 1.83$\pm$0.01. In the period January 2009-March 2009, $V_P/V_S$ is 1.84$\pm$0.01. This last value slightly increases to 1.86$\pm$0.01 in the time interval March 31-April 6, 2009. From the mainshock occurrence to April 30, $V_P/V_S$ reaches a value of 1.95$\pm$0.01 (Fig. 5). In conclusion, $V_P/V_S$ gently increases from October 2008 to April 6 2009, and abruptly changes from the mainshock (April 6, 01:32) to April 30 (Fig. 5).

In order to study the $V_P/V_S$ changes along different strikes, we selected data relative to two different structural paths (Fig. 6): a) a NW-SE orientation, which coincides with the preferred strike of the Aterno faults and aftershock alignment (AQU-FAGN); b) a NE-SW orientation (AQU-FIAM) roughly transversal to the previous one. There is a large increase of $V_P/V_S$ estimated along the path AQU- FAGN from the January 2009-March 2009 period to the following March-April 6 2009 (Fig. 6). In particular, $V_P/V_S$ increases from 1.87$\pm$0.01 to 1.97$\pm$0.02 for the AQU-FAGN path. On the contrary, $V_P/V_S$ on the AQU-FIAM path is nearly constant with values of 1.77-1.78.

## 6. Discussion

### *6.1 The activated faults and kinematics*

The distribution of the April 2009 L'Aquila seismic sequence (Fig. 3) indicates that earthquakes occurred along three main structures:

A) a 15 km long, NW-SE striking, about 50° SW-dipping structure (April 6 mainshock and aftershocks) from which a 30° SW dipping structure departs at about 7-8 km of depth (sections 2 and 3 in Fig. 3b). The seismicity mainly occurs at the boundary between an upthrusted block of the metamorphic basement and the overlying nappes and folds of the chain, in an area where the uprising of the mantle wedge occurs (section 3 in Fig. 3b) [*Ghisetti and Vezzani*, 2002]. The location of the aftershocks overlaps the Paganica fault trace (Pf in Fig. 3b), as also found in other studies [*Chiarabba et al.*, 2009]. The surface ruptures associated to the April 6 mainshock along the Paganica fault [*Emergeo Working Group*, 2010] strongly supports this interpretation. Our data show, however, that the Gran Sasso thrust was likely reactivated (GSt in Fig. 3b). The rake distribution from the focal mechanisms (Fig. 4) indicates prevailing normal slips along NW-SE striking, with 30° to 50° SW dipping rupture planes. Therefore, both the Gran Sasso thrust, whose activity dates back to pre-Pliocene times, and the Quaternary Paganica fault were reactivated as normal faults during the April 2009 sequence. The foreshock distribution indicates that the early stage of the rupture process occurred on the Paganica fault, and in particular, on its hanging wall. This observation well agrees with numerical models on the early stages of coseismic fault activation [*Zhang and Sanderson*, 1996a]. Such models show that, within a pre-fractured medium crossed by a normal fault, the rupture affects both the fault zone and the hanging wall. As the April 2009 sequence evolves in time, aftershocks concentrate in the fault zone and in its footwall.

B) a 20 km long, NNW-SSE striking, 4-5 km wide rupture zone, confined between 6 and 12 km of depth, is evidenced by the April 7 2009 ($M_w$= 5.6) larger aftershock and associated seismicity (Fig. 3a and section 4 in Fig. 3b). On the surface, faults possibly related to this rupture are lacking.

A gap in seismicity exists between the April 7 ($M_w$=5.6) nucleation, which occurred at ~14 km of depth, and the related cluster (section 4 in Fig. 3b). This gap could be due to an aseismic shearing zone. Aseismic shearing may occur in the middle-lower continental crust, where it is generally associated to fluid trapped by impermeable layers [*Goto et al.*, 2005]. In the L'Aquila area (Fig. 1b), evidence of pressurized, mantle-derived fluids is given by the high $CO_2$ release (1-5 $10^6$ mol $km^{-2}yr^{-1}$) [*Chiodini et al.*, 2000], while the impermeable layer could be represented by the Permo-Triassic evaporites, occurring between the metamorphic basement of the chain and the overlying nappes, at depth between 12 and 16 km [*Patacca et al.*, 2008]. As a preliminary hypothesis, we suggest that aseismic shearing occurred in the seismic gap area between the April 7 ($M_w$=5.6) event and the overlying aftershock volume.

C) Two subvertical, 15-20 km long NW-SE striking structures extending between 3-4 km and about 12 km of depth are depicted by the April 9 2009 ($M_w$= 5.4) event and its aftershocks (section 1 in Fig. 3b). Evidence of surface faulting for these structures is lacking [*Atzori et al.*, 2009; *Emergeo Working Group*, 2010].

The low number of seismic events among the seismogenic structures A, B, and C, whose activity was continuous from April 6 to the end of April 2009, indicates the lack of mature transfer zones among the main NW-SE to NNW-SSE striking ruptures. According to structural models of normal fault networks [*Peacock*, 2002], this feature suggests an early stage of formation for the L'Aquila seismogenetic fault network. On the basis of above data and observations, we propose that the L'Aquila sector of the Apennines is at a less mature stage with respect to the southern sector of the chain, where, instead, seismicity on transfer structures among the main NW-SE faults was recognized [*Milano et al.*, 2002]. The lower structural maturity of the central Apennines could be due to a relative lower extension rate of the central sector of the chain, which is roughly about 3 mm/yr , whereas values up to 5 mm/yr characterize the southern Apennines [*Hunstad et al.*, 2003].

The focal mechanisms of the L'Aquila events with $M_w$> 5 (Fig. 3), as well as the results of the stress field analysis (Fig. 4b) show that the recognized A, B and C seismogenetic structures moved in response to a NE-SW extension, which is that acting at regional scale, as previously reported [*Montone et al.*, 2004]. Therefore, the fault kinematics and the stress field of the L'Aquila sequence are consistent with the present-day tectonic configuration of the Apennines [*Chiarabba et al.*, 2005; *Mantovani et al.*, 2009]. *Patacca et al.* [2008] suggest that the NE-SW extension and Apennines seismicity are related to the gravity adjustment of the upper crust due to an out-of-sequence propagation of the active thrusts, i.e. compression, at depth. The focal mechanisms of the L'Aquila 2009 events do not evidence active thrusting (compression), showing normal and minor oblique slip solutions (Fig. 4). On the basis of our results, we exclude the hypothesis by *Patacca et al.* [2008] on the occurrence of active compression within the axial sector of central Apennines.

*6.2 Evidence of fluids and preferred fluid path*

Some authors [*Ghisetti and Vezzani*, 2002, *Chiodini et al.*, 2004; *Ventura et al.,* 2007] suggest that the seismotectogenesis of the Apennines is related to the uprising of mantle derived fluids. In addition, *Miller et al.* [2004] propose that the aftershocks of the Umbria-Marche 1997 sequence in northern Apennines were related to the release of overpressurized $CO_2$. At L'Aquila, the presence of fluids was evidenced by a drop in the intensity of the radio signal between March 31 and April 1 2009 [*Biagi et al.*, 2009]. Such drop was not related to transmission errors, but was produced by electromagnetic particles and gas emissions in the area of preparation of the April 6 mainshock [*Biagi et al.*, 2009].

The $V_P/V_S$ value estimated for the foreshocks and aftershocks of the L'Aquila 2009 sequence is between 1.83 and 1.95 and increases from October 2008 to April 2009 (Fig. 5). $V_P/V_S$ =1.83 was also found in previous studies on central Apennines [*Bagh et al.*, 2007], whereas $V_P/V_S$=1.95 is anomalously high, and it is consistent with values estimated in fluid-rich zones [*Zhao and Negishi*, 1998; *Husen and Kissling*, 2001]. In particular, a $V_P/V_S$ value of 1.9 was found in northern Apennines and was interpreted to reflect the presence of pressurized fluids in the crust [*Moretti et al.*, 2009]. We conclude that fluids were present within the seismogenic volume of the L'Aquila 2009 sequence.

Laboratory and borehole experiments proved $V_P/V_S$ to increase with the concentration of fluid saturated cracks [*Moos and Zoback*, 1983], and several studies show anomalous changes in $V_P/V_S$ during earthquakes [*Nadeau et al.*, 1994; *Chen et al.*, 2001]. An increase in $V_P/V_S$ may evidence the presence of fluids in the seismogenic faults [*Eberhart-Phillips and Michael*, 1993, *Zhao et al.*, 1996]. Therefore, the raise in seismicity rate and $V_P/V_S$ during the L'Aquila 2009 sequence (Fig. 5) could be due to an increase of cracking associated to fluid migration. The occurrence of structurally controlled, i.e. NW-SE to NNW-SSE striking, subvertical clouds of events (sections 1, 3 and 4 in Fig. 3b) is also compatible with a migration of fluids, being these vertical clouds typical of fluid-induced seismicity [*Shapiro et al.*, 1997; 2003], as also recognized in sequences in the northern Apennines associated to fluid movements [*Calderoni et al.*, 2009].

Data reported in Fig. 6 show a significant increase of $V_P/V_S$ (from 1.87 to 1.97) along the AQU-FAGN path, which is parallel to the NW-SE striking Paganica fault. Therefore, the seismogenic volume is characterized by a time-and space-dependent anisotropy, which can reflect the preferred migration of fluids along the strike of the rupture zone. This interpretation well agrees with numerical models [*Zhang and Sanderson*, 1996b] and field observations on the migration of fluids in active faults [*Sibson*, 2000, and reference therein]. Such models predict that the permeability of faults increases along the direction of the maximum horizontal stress $\sigma_H$ and fluid flow is allowed along this direction. In an extensional regime, $\sigma_H=\sigma_2$ and fluids preferably migrate along planes containing $\sigma_2$. In the L'Aquila case, $\sigma_2$ is parallel to the preferred NW-SE fault strike (Fig. 4). In conclusion, the increase of $V_P/V_S$ along the AQU-FAGN path (Fig. 6) results from the passage of fluids along the NW-SE fault strike possibly allowed by the higher permeability of the faulted rocks. This interpretation is consistent with results from previous studies, which show that lateral variations of $V_P/V_S$ are sensitive to the faulting property [*Eberhart-Phillips and Michael*, 1998; *Graeber and Asch*, 1999; *Gentile et al.*, 2000]. As concerns the role of fluids in activating pre-existing structures, we remark that while static stress interaction explains failure between collinear segments of strike-slip faults or collateral segments of normal faults, it does not hold for the activation of collinear normal faults [*Nostro et al.*, 1997]. According to *Noir et al.*, [1997] and *Sibson*

[2000], the interaction and activation in short times (few hours) of collinear normal faults like those activated during the L'Aquila sequence may arise from the propagation of a fluid pressure wave through an anisotropic fractured rock-mass.

*6.3 Pore pressure diffusion and permeability*

*Shapiro et al.* [1997, 2003] propose that the triggering of seismicity and the consequent spatio-temporal evolution can be analyzed in terms of pore-pressure relaxation in media with (an)isotropic hydraulic diffusivity. In a plot distance of the pressure front from the triggering front versus time, a parabolic-like envelope of cloud of events is recognized when a diffusion-like process operates. In a poroelastic medium, the extension of the rupture zone can be approximated, by the theoretical curve $r=(4\pi Dt)^{1/2}$, where the distance $r$ of the pressure front from the fluid source (triggering front) is as a function of the diffusivity $D$ and time $t$ [*Shapiro et al.*, 1997]. We analyzed a) the foreshock distribution from March 30 2009 to April 6 2009 before the mainshock because of a marked increase in the cumulative number of events (Fig. 5), and b) the aftershocks from the mainshock to April 30 2009. Both the foreshocks and the aftershocks used in this analysis are the relocated events described in section 3. In a distance-versus-time ($r$-$t$) diagram, we identify a triggering front with a diffusivity of 4.5 $m^2/s$ for the foreshocks (Fig. 7a), whereas the aftershocks give a diffusivity of 80 $m^2/s$ (Fig. 7b). We used a linearized inversion procedure to fit the equation $r=(4\pi Dt)^{1/2}$ to hypocenter data following *Saccorotti et al.* [2002]. In particular our procedure for fitting the above equation is to select the farthest earthquakes that occurred in consecutive, not overlapping times. We remark that, while a clear diffusion-like seismicity is depicted by the aftershocks, the low number of foreshocks does not allow us to unequivocally identify a fluid-controlled seismicity. In any case, the determined $D$ values are within those reported in literature [e.g. *Roeloffs*, 1996; *Talwani et al.*, 2007] with $D$=80 $m^2/s$ representing an upper limit [*Roeloffs*, 1996]. This latter, large value of $D$ implies a high permeability $k$ of the crustal rocks, being $D$ proportional to $k$ [e.g. *Talwani et al.*, 2007] through the relation:

$$k = D\eta\Phi\beta \qquad (1)$$

where $\eta\Phi\beta$ are the fluid viscosity, the porosity of the rock and the compressibility of fluid, respectively. In the case of water, $\eta = 10^{-3}$ Pa s, $\beta = 3 \cdot 10^{-9}$ Pa$^{-1}$. $\Phi$ is set to 0.07 [*Iscan et al.*, 2006]. In presence of $CO_2$, the product $\eta\beta$ does not change because $CO_2$ at source depth is in a supercritical state, and it is ten times more compressible than water and ten time less viscous [*Miller et al.*, 2004]. Using the above selected parameters and equation 1, we obtain $k = 5.6 \cdot 10^{-12}$ m$^2$, which has the significance of an order of magnitude estimate and refers to a dynamic, seismogenic permeability [*Talwani et al.*, 2007]. This value is two order of magnitude larger than that measured in fault gauges relative to faults outcropping in the Abruzzo area ($k \leq 10^{-14}$ m$^2$) [*Agosta et al.*, 2007]. Besides, the estimated value of permeability is consistent with the gas permeability values measured in carbonatic rocks ($k$ up to $10^{-12}$ m$^2$) [*Lucia et al.*, 1999] and in laboratory experiments on limestones under stress conditions ($k$ up to 1.3 $10^{-12}$ m$^2$) [*Iscan et al.*, 2006].

*6.4 Fluid pressure, stress regime and comparison with other fluid-rich structural settings*

The above summarized results indicate that fluid pressure played an important role in the April 2009 seismicity. In order to determine the fluid pressure necessary to activate the A, B, and C L'Aquila structures (section 6.1), we calculate the stress difference $\sigma_1$-$\sigma_3$ required to fracture the rock along a plane with ideal orientation and compare this value with that required for slip along different pre-existing planes of weakness of variable orientation, following the approach of *Yin and Ranalli* [1992] as implemented in the ReActiva software [*Alaniz-Alvares and Tolson*, 2000]. The input data include the stress ratio $\Phi$ the rock cohesion $c$, the coefficient of internal friction $\mu$, and the pore fluid factor $\lambda = P_f/(\rho g z)$, with $P_f$=fluid pressure, $\rho$=rock density, $g$= gravity, and $z$=depth. In a normal stress regime, $\rho g z = \sigma_1$. For the

April 2009 L'Aquila sequence, we adopt a normal stress regime with a NE-SW striking $\sigma_3$ (Fig. 4b), and set: $\Phi$=0.65 (see Fig. 4), *c*=0 assuming that the ruptures occur along pre-existing planes of weakness (for the intact rock, *c*=10 MPa), $\mu$=0.6 [*Sibson*, 2000], $\rho$=2650 kg/m$^3$ and *z*=10 km (Fig. 3). Results are shown in Fig. 8, where the contour plot (gray areas) of the poles to planes is reported at different $\lambda$ as a function of the ratio *T* between the shear and normal stress [*Morris et al.*, 1996]. In this plot, *T/Ts* gives the slip tendency of each plane being *Ts* the maximum calculated *T*. The poles to the inferred activated structures A (NW-SE strike; dip 45°, Paganica fault and 30°, SW dipping, re-activated Gran Sasso thrust), B (NW-SE strike, dip 80°-90°) and C (NNW-SSE strike, dip 80°-90°) are also reported. Results show that for $\lambda$=0.4, none of the A, B and C poles falls in the field of the slipping faults. For $\lambda$ =0.6, the NW-SE and NNW-SSE striking structures with dip $\geq$45° fall in the contour plot with *T/Ts* $\geq$0.8, whereas the structure with dip=30° is in the field with *T/Ts* $\leq$0.1%. For $\lambda$=0.8, all the inferred rupture planes fall in the area with *T/Ts* $\geq$0.8%. These results suggest a suprahydrostatic fluid pressure. We conclude that $\lambda$ values between 0.6 and 0.8 are necessary to explain the (re)activation of the April 2009 L'Aquila structures. Taking into account the relation between $\lambda$ and $P_f$, we estimate a $P_f$ between 155 and 207 MPa at 10 km depth. The largest $P_f$ value is consistent with that calculated to activate thrusts in the outer sector of Apennines ($P_f$ =215 MPa at 10 km depth from *Calderoni et al.*, 2009), where a compressive stress regime exists. We propose that, despite the different stress regime and fluid sources, i.e. methane and petroleum in the outer sector [*Calderoni et al.*, 2009] and mantle-derived $CO_2$ in the axial sector [*Chiodini et al.*, 2004], the fluid pressure below these two sectors of Apennines chain is nearly constant. This implies the existence of overpressurized reservoirs in which, after an earthquake, $P_f$ possibly decreases due to the upward migration of fluids along the activated fault(s). The fluid involvement in fault systems characterized by a normal stress regime like that recognized in the L'Aquila region may differ from that in strike-slip regimes, e.g. the Bohai Bay Basin system (China). Here, mantle-derived fluids migrate along subvertical faults that cross the basement, and, in particular, at the intersection of faults, where fluid pressure is low because of the continuous gas release [*Zhang et al.*, 2008].

### *6.5 Geodynamic implications*

The April 2009 L'Aquila seismicity evidences suprahydrostatic overpressures approaching lithostatic values in a structurally controlled intra-mountain basin (Figs. 2 and 8). As noticed by *Sibson* [2000], the sustainability of large fluid pressures in extensional regimes is a still debated question, however, our data show that, in central Apennines, relatively large fluid pressures are required to activate faults that may produce $M_w$=5-6 earthquakes. According to the available geochemical [*Chiodini et al.*, 2004; *Frezzotti et al.*, 2009] and geodynamic [*Ghisetti and Vezzani*, 2002; *Ventura et al.*, 2007] models of the Apennines, the source of fluids may be the metasomatized mantle wedge, which releases carbon dioxide in the overlying continental crust. Our data suggest that pressurized fluid traps within the crust may be confined by structural (pre-existing thrusts and folds within the carbonates) and/or lithological (impermeable layers like the Permo-Triassic evaporites) discontinuities. This geodynamic picture may explain why the seismicity of the Apennines concentrates in the upper plate and not in the downgoing plate or in both the downgoing and overriding plates, as observed in the majority of subduction settings [*Stern*, 2002].

## **7. Conclusions**

The results of this study may be summarized in the following main points:

(a) The April 2009 L'Aquila seismic activity developed along three main, quasi-collinear structures striking NW-SE to NNW-SSE that moved in response to a NE-SW extension. One of these structures corresponds to an outcropping normal fault (Paganica). A portion of the Gran Sasso thrust, at the junction with the fault responsible of the earthquake, was also reactivated with a normal mechanism. The structural maturity of this system of structures is lower than that displayed by similar systems in southern Apennines, which are affected by a larger strain rate.

(b) $V_P/V_S$ increases progressively from October 2008 to the April 6 2009 mainshock along a NW-SE preferred strike This increase is related to an increment of pore fluid pressure. The $V_P/V_S$ spatial anisotropy is related to the movement of fluids along fault planes.

(c) Pore pressure diffusion is the main mechanism controlling the space-time distribution of aftershocks. An increase of fluid pressure due to the upward migration of fluids induced an increase of pressure in the connected pore space, which includes pores and cracks. By increasing the pore pressure the effective normal stress and cohesion decrease. This leads to sliding along pre-existing subcritical cracks and to the initiation of the rupture. Hydraulic diffusivity is about 80 $m^2/s$, which represents an upper bound for the diffusivity of crustal rocks and which probably reflects the involvement of gas ($CO_2$) from deep source. The seismogenic permeability is in the order of $10^{-12}$ $m^2$. Suprahydrostatic pressure conditions were required to activate the L'Aquila seismic sequence with $P_f$ values up to about 200 MPa at 10 km of depth.

(d) Overpressurized traps along pre-existing structural and/or lithological discontinuities at the lower-upper crust boundary are required to explain the calculated $P_f$. Such traps may represent the storage zone of $CO_2$-rich fluids uprising from the underlying, metasomatizied mantle wedge. These traps, which are easy to form in an extensional regimes like that acting in the L'Aquila area, are difficult to develop in strike-slip regimes, where sub-vertical faults may cross the entire crust.

(e) In the L'Aquila zone of central Apennines, fluids may activate faults producing earthquakes up to $M_w$=5-6. The April 2009 L'Aquila sequence occurred on the axial zone of the chain, i.e. in the overriding plate of the Apennines subduction system, and not in the downgoing plate, as, on the contrary, usually recognized in subduction zones.

Such features suggest that deep fluids more than tectonic stress control the seismotectogenesis of accretionary wedges.

**Acknowledgments.** Robert Herrmann is gratefully thanked to give public access to the online focal mechanisms of the L'Aquila 2009 sequence. Discussions with G. Chiodini , R. Devoti and F. P. Lucente and comments by the Associate Editor, an anonymous reviewer and Zhengfu Guo helped to improve the manuscript. Some of the figures were done using GMT [*Wessel and Smith*, 1991]. G. V. was supported by the IYPE project ‘Creep’.

## References

Agosta, F., M. Prasad, and A. Aydin (2007), Physical properties of carbonate fault rocks, Fucino basin (central italy): implications for fault seal in platform carbonates, *Geofluids*, 7, 19–32.

Alaniz-Alvares S., and G. Tolson (2000), Assessing Fault Reactivation with the ReActiva Program. *Journal of Geoscience Education*, 48, 651-657.

Atzori, S., I. Hunstad, M. Chini, S. Salvi, C. Tolomei, C. Bignami, S. Stramondo, E. Trasatti, A. Antonioli, and E. Boschi (2009), Finite fault inversion of DInSAR coseismic displacement of the 2009 L'Aquila earthquake (central Italy), *Geophys. Res. Lett.*, 36, L15305, doi:10.1029/2009GL039293.

Bagh, S., L. Chiaraluce, P. De Gori, M. Moretti, A. Govoni, C. Chiarabba, P. Di Bartolomeo, and M. Romanelli (2007), Background seismicity in the Central Apennines of Italy: The Abruzzo region case study, *Tectonophysics*, 444, 1-4, 80-92.

Biagi, P.F., L. Castellana, T. Maggipinto, D. Loiacono, L. Schiavulli, T. Ligonzo, M. Fiore, E. Suciu, and A. Ermini (2009), A pre seismic radio anomaly revealed in the area where the

Abruzzo earthquake (M=6.3) occurred on 6 April 2009, *Nat. Hazards Earth Syst. Sci.*, 9, 1551–1556.

Blumetti, A. M., M. Di Filippo, P. Zaffiro, P. Marsan, and B. Toro (2002), Seismic hazard of the city of L'Aquila (Abruzzo - Central Italy): new data from geological, morphotectonic and gravity prospecting analysis, *Studi Geologici Camerti,* 1, 7–18.

Calderoni G., R. Di Giovambattista, P. Burrato, and G. Ventura (2009), A seismic sequence from Northern Apennines (Italy) provides new insight on the role of fluids in the active tectonics of accretionary wedges, *Earth and Planetary Science Letters,* doi:10.1016/j.epsl.2009.02.015.

Castello, B., G. Selvaggi, C. Chiarabba, and A. Amato (2005), CSI Catalogo della sismicità italiana 1981–2002, versione 1.0. INGV-CNT, Roma

Chen, C.H., W.H. Wang, and T.L. Teng (2001), 3D velocity structure around the source area of the 1999 Chi-Chi, Taiwan, earthquake: Before and after the mainshock, *Bull. Seismol. Soc. Am.*, 91, 5, 1013-1027.

Chiarabba, C., L. Jovane, and R. Di Stefano (2005), A new view of Italian seismicity using 20 years of instrumental recordings, *Tectonophysics*, 395, doi:10.1016/j.tecto.2004.09.013.

Chiarabba, C., A. Amato, M. Anselmi, P. Baccheschi, I. Bianchi, M. Cattaneo, G. Cecere, L. Chiaraluce, L., M.G. Ciaccio, P. De Gori, G. De Luca, M. Di Bona, R. Di Stefano, L. Faenza, A. Govoni, I. Improta, F. P. Lucente, A. Marchetti, L. Margheriti, F. Mele, A. Michelini, G. Monachesi, M. Moretti, M. Pastori, N. Piana Agostinetti, D. Piccinini, P. Roselli, D. Seccia, and L. Valoroso (2009), The 2009 L'Aquila (central Italy) $M_W$ 6.3 earthquake: Main shock and aftershocks, *Geophys. Res. Lett.*, 36, L18308, doi:10.1029/2009GL039627.

Chiodini, G., F. Frondini, C. Cardellini, F. Parello, and L. Peruzzi (2000), Rate of diffuse carbon dioxide Earth degassing estimated from carbon balance of regional aquifers: The case of central Apennines, Italy, *J. Geophys. Res.*, 105, 8423– 8434.

Chiodini, G., C. Cardellini, A. Amato, E. Boschi, S. Caliro, F. Frondini, and G. Ventura (2004), Carbon dioxide Earth degassing and seismogenesis in central and southern Italy, *Geophys. Res. Lett.*, 31, L07615, doi:10.1029/2004GL019480.

Di Luzio E., G. Mele, M. M. Tiberti, G. P. Cavinato, and M. Parotto (2009), Moho deepening and shallow upper crustal delamination beneath the central Apennines, *Earth Planet. Sci. Lett.*, doi:10.1016/j.epsl.2008.09.018.

Di Stefano, R., C. Chiarabba, F. P. Lucente, and A. Amato (1999), Crustal and uppermost mantle structure in Italy from the inversion of P-wave arrival times: geodynamic implications, *Geophys. J. Int.*, 139, 483–498.

Doglioni C. (1991), A proposal of kinematic modelling for W-dipping subductions - Possible applications to the Tyrrhenian - Apennines system, *Terra Nova*, 3, 4, 423-434.

Doglioni, C. (1995), Geological remarks on the relationships between extension and convergent geodynamic settings, *Tectonophysics* 252, 253–268.

Eberhart-Phillips, D., and A. J. Michael (1993), Three-dimensional velocity structure and seismicity in the Parkfield region, central California, *J. Geophys. Res.*, 98, 15,737-15,758.

Eberhart-Phillips, D., and A. J. Michael (1998), Seismotectonics of the Loma Prieta, California, region determined from three-dimensional Vp, Vp/Vs, and seismicity, *J. Geophys. Res.*,103, B9, 21099-21120.

Emergeo Working Group (2010), Evidence for surface rupture associated with the Mw 6.3 L'Aquila earthquake sequence of April 2009 (central Italy), *Terra Nova*, 1, 22, doi:10.1111/j.1365-3121.2009.00915.x.

Frezzotti M.L., A. Peccerillo, and G. Panza (2009), Carbonate metasomatism and CO2 lithosphere-asthenosphere degassing beneath the Western Mediterranean: An integrated model arising from petrological and geophysical data, *Chemical Geology*, 262, 108-120.

Galadini, F., and P. Galli (2000), Active tectonics in the central Apennines (Italy) -input data for seismic hazard assessment, *Nat. Haz.,* 22, 225–270.

Gentile G.F, G. Bressan, L. Burlini, and R. De Franco (2000), Three dimensional Vp and Vp/Vs models of the upper crust in the Friuli area (northeastern Italy), *Geophys. J. Int.*, 141, 457-478.

Ghisetti, F., and L. Vezzani (1999), Depth and modes of Pliocene–Pleistocene crustal extension of the Apennines (Italy), *Terra Nova*, 11, 67–72.

Ghisetti, F., and L. Vezzani (2002), Normal faulting, transcrustal permeability and seismogenesis in the Apennines (Italy), *Tectonophysics*, 348, 155 – 168.

Goto, T., Y. Wada, N. Oshiman, and N. Sumitomo (2005), Resistivity structure of a seismic gap along the Atotsugawa Fault, Japan, *Phys. Earth Planet. Int.*, 148, 55-72

Graeber, F. M., and G. Asch (1999), Three-dimensional models of P wave velocity and P-to-S velocity ratio in the southern central Andes by simultaneous inversion of local earthquake data, J. Geophys. Res., B104-9, 20,237-20,256.

Hunstad, I., G. Selvaggi, N. D'Agostino, P. England, P. Clarke, and M. Pierozzi (2003), Geodetic strain in peninsular Italy between 1875 and 2001, *Geophys. Res. Lett.*, 30(4), 1181, doi:10.1029/2002GL016447

Husen, S., and E. Kissling (2001), Postseismic fluid flow after the large subduction earthquake of Antofagasta, Chile, *Geology*, 29, 847–850.

Iscan, A.G., M. V. Kök, and A. S. Bagcı (2006), Estimation of permeability and rock mechanical properties of limestone reservoir rocks under stress conditions by strain gauge, *J. Pet. Sci. Eng.,* 53, 13–24.

Klein, F. (2000), HYPOINVERSE-2000, a FORTRAN program to solve for earthquake locations and magnitudes, *U.S. Geol. Surv. Open File Rept.*, 02-171.

Lavecchia G., P. Boncio, and N. Creati (2003), A lithospheric scale seismogenic thrust in central Italy, *Journal of Geodynamics*, 36, 79-94.

Lucia, J (1999), Carbonate Reservoir Characterization: An Integrated Approach, 2nd edition, Springer-Verlag Berlin, 336 p.

Malinverno A., and W. B. F. Ryan (1986), Extension in the Tyrrhenian sea and shortening in the Apennines as result of arc migration driven by sinking of the lithosphere, *Tectonics*, 5, 227-245.

Mantovani E., D. Babbucci, C. Tamburelli, and M. Viti (2009), A review on the driving mechanism of the Tyrrhenian-Apennines system: Implications for the present seismotectonic setting in the Central-Northern Apennines, *Tectonophysics*, 476, 22-40.

Mele, G., A. Rovelli, D. Seber, and M. Barazangi (1996), Lateral variations of Pn propagation in Italy: Evidence for a high attenuation zone beneath the Apennines, *Geophys. Res. Lett.*, 7/23, 709-712.

Michael, A.J. (1987), Determination of stress from slip data: faults and folds, *J. Geophys. Res.*, 89, 11517–11526.

Milano, G., G. Ventura, and R. Di Giovambattista (2002), Seismic evidence of longitudinal extension in the Southern Apennines chain (Italy): The 1997–1998 Sannio-Matese seismic sequence, *Geophys. Res. Lett.*, 29(20), 2004, doi:10.1029/2002GL015188.

Miller, S. A., C. Collettini, L. Chiaraluce, M. Cocco, M. Barchi, M., and B. J. P. Kaus (2004), Aftershocks driven by a high-pressure $CO_2$ source at depth, *Nature*, 427, doi:10.1038/nature2251.

Montone, P., M. T. Mariucci, S. Pondrelli, and A. Amato (2004), An improved stress map for Italy and surrounding regions (central Mediterranean), *J. Geophys. Res.*, 109, doi:10.1029/2003JB002703.

Moos, D., M. D. Zoback (1983), In situ studies of velocity in fractured crystalline rocks, *J. Geophys. Res.*, 88, 2345– 2358.

Moretti M., P. De Gori, and C. Chiarabba (2009), Earthquake relocation and three-dimensional Vp and Vp/Vs models along the low angle Alto Tiberina Fault (Central Italy): evidence for fluid overpressure, *Geophys. J. Int.*, 176, 833–846.

Morris, A., D. A. Ferrill, and D. B. Henderson (1996), Slip-tendency analysis and fault reactivation, *Geology,* 24, 275–278.

Nadeau, R., M. Antolik, P. Johnson, W. Foxall, and T. V. McEvilly (1994), Seismological studies at Parkfield III: microearthquake clusters in the study of fault-zone dynamics, *Bull. Seism. Soc. Am.*, 83, 247 –263.

Noir, J., E. Jacques, S. Bekri, P. M. Adler, P. Tapponier, and G. C. P. King (1997), Fluid flow triggered migration of events in the 1989 Dobi earthquake sequence of Central Afar, *Geophys. Res. Lett.*, 24, 2335-2338.

Nostro, C., M. Cocco, and M. E. Belardinelli (1997), Static stress changes in extensional regimes: an application to Southern Apennines, Italy, *Bull. Seism. Soc. Am.*, 87, 234-248.

Patacca, E., P. Scandone, E. Di Luzio, G. Cavinato, and M. Parotto (2008), Structural architecture of the central Apennines: interpretation of the CROP 11 seismic profile from the Adriatic coast to the orographic divide, *Tectonics*, 27, 3, doi:10.1029/2005TC001917.

Peacock, D. C. P. (2002), Propagation, interaction and linkage in normal fault systems, *Earth-Science Rev.*, 58, 1-2, 121-142.

Pino, N. A., and F. Di Luccio (2009), Source complexity of the 6 April 2009 L'Aquila (Central Italy) earthquake and its strongest aftershock revealed by elementary seismological analysis, *Geophys. Res. Lett.*, doi:10.1029/2009GL041331.

Pizzi, A., and F. Galadini (2009), Pre-existing cross-structures and active fault segmentation in the northern-central Apennines (Italy), *Tectonophysics*, 476, doi:10.1016/j.tecto.2009.03.018.

Roeloffs, E. (1996), Poroelastic techniques in the study of earthquake related hydrologic phenomena, *Adv. Geophys.*, 37, 136– 195.

Saccorotti, G., G. Ventura, and G. Vilardo (2002), Seismic swarms related to diffusive processes: The case of Somma-Vesuvius volcano, Italy, *Geophysics*, 67(1), 199–203.

Satolli, S., and F. Calamita (2008), Differences and similarities between the central and the southern Apennines (Italy): Examining the Gran Sasso versus the Matese-Frosolone salients using paleomagnetic, geological, and structural data, *J. Geophys. Res.*, 113, B10101, doi:10.1029/2008JB005699.

Shapiro, S.A., E. Huenges, and G. Borm (1997), Estimating the crust permeability from fluid injection-induced seismic emission at the KTB site, *Geophys. J. Int.*, 131, F15–F18.

Shapiro, S.A., R. Patzig, E. Rothert, and J. Rindschwentner (2003), Triggering of seismicity by pore pressure perturbations: permeability related signatures of the phenomenon, *Pure Appl. Geophys.*, 160, 1051–1066.

Sibson R.H. (2000), Fluid involvement in normal faulting, *Journal of Geodynamics,* 29, 469-499.

Stern, R. J. (2002), Subduction zones, *Rev. Geophys.*, 40(4), 1012, doi:10.1029/2001RG000108.

Talwani P., L. Chen, and K. Gahalaut (2007), Seismogenic permeability, ks, *J. Geophys. Res.*, 112, B07309, doi:10.1029/2006JB004665.

Tertulliani, A., A. Rossi, L. Cucci, and M. Vecchi (2009), L'Aquila (Central Italy) earthquakes: the predecessors of the April 6, 2009 event, *Seism. Res. Lett.*, 80, 6, 972-977, doi: 10.1785/gssrl.80.6.972.

Ventura, G., F. R. Cinti, F. Di Luccio, and N. A. Pino (2007), Mantle wedge dynamics vs crustal seismicity in the Apennines (Italy), *Geochem. Geophys. Geosys.*, 8, doi:10.1029/2006GC001421.

Wadati, K. (1933), On the travel time of earthquake waves. Part II, *Geophys. Mag.*, 7, 101–111.

Waldhauser, F., and W. L. Ellsworth (2000), A double-difference earthquake location algorithm: method and application to the Northern Hayward Fault, California, *Bull. Seismol. Soc. Am.*, 90, 1353–1368.

Wessel, P., and W. H. F. Smith (1991), Free software helps map and display data, *Eos Trans. AGU*, 72, 441, 1991.

Yin, Z.M., and G. Ranalli (1992), Critical stress difference, fault orientation and slip direction in anisotropic rocks under non-Andersonian stress systems, *J. Struct. Geol.*, 14 237–244.

Zhang, X., and D. J. Sanderson (1996a), Numerical modelling of the effects of fault slip on fluid flow around extensional faults, *J. Struct. Geol.*, 18, 109-122.

Zhang, X., and D. J. Sanderson (1996b), Effects of stress on the two-dimensional permeability tensor of natural fracture networks, *Geophys. J. Int.*, vol. 125, issue 3, pp. 912-924.

Zhang, T., M. Zhang, B. Bai, X. Wang, and L. Li (2008), Origin and accumulation of carbon dioxide in the Huanghua depression, Bohai Bay Basin, *Chin. AAPG Bull.* 92, 341–358.

Zhao, D., H. Kanamori, H. Negishi, and D. Wiens (1996), Tomography of the source area of the 1995 Kobe earthquake: Evidence for fluids at the hypocenter?, *Science*, 274, 1891–1894.

Zhao, D., and H. Negishi (1998), The 1995 Kobe earthquake: seismic image of the source zone and its implications for the rupture nucleation, *J. Geophys. Res.*, 103, 9967–9986.

## Figure captions

**Figure 1.** a. Structural scheme of Italy and seismicity distribution (red dots) from 1981 to 2002 [*Castello et al.*, 2005]. b. Geological sketch map of the Abruzzi region [modified from *Satolli and Calamita*, 2008]. $CO_2$ gas fluxes are from *Chiodini et al.* [2000]. The low Vp zone at depth > 20 km is from *Di Stefano et al.* [1999]. c. Crustal profile from CROP 11 data [modified from *Ghisetti and Vezzani*, 2002].

**Figure 2.** Structural map of the L'Aquila area with evidenced Quaternary faults [modified from *Emergeo Working Group* 2010]. The historical earthquakes are from http://emidius.mi.ingv.it/CPTI08/.

**Figure 3.** a. Time and epicentral distribution of the April 2009 L'Aquila seismic sequence and its foreshocks. Stars indicate the foreshocks occurred from October 1 2008 to April 6 2009 (01h20m). Focal mechanisms of the events with $M_w$ greater than 5 (black beach balls) and of the foreshocks (gray beach balls) are from http://eqinfo.eas.slu.edu/Earthquake_Center/MECH.IT/. Faults are from Fig. 2. b. Cross-sections of the seismicity depicted in Fig. 3a, with black dots indicating the aftershocks and the red stars indicating the foreshocks. The yellow circle and star, and the green diamond correspond to the events marked in Fig. 3a. Quaternary faults (red segments, dashed when the dip is inferred) are from Fig. 3a, while the trace of the Gran Sasso thrust (blue segments in profiles 2 and 3) is from *Satolli and Calamita* [2008]. In the profile 3, the crustal layers are from Fig. 1c.

**Figure 4.** Strike, dip and rake distribution of focal mechanism nodal planes (data from http://eqinfo.eas.slu.edu/Earthquake_Center/MECH.IT/). B. Density distribution of poles to nodal planes. C. Results of the stress field analysis [*Michael*, 1987] on 35 focal mechanisms

of earthquakes with $M_w$>3 occurred in April 2009. The parameter $\phi=(\sigma_2-\sigma_3)/(\sigma_1-\sigma_3)$ , with the principal stress axes $\sigma_1 \geq \sigma_2 \geq \sigma_3$.

**Figure 5.** Time versus cumulative number of earthquakes for the period October 2008-April 2009, including the mainshock of April 6 2009 (yellow star). Vp/Vs calculated for the different time intervals marked by jumps in the cumulative number of events are reported with different colors. Vp/Vs values were determined using the stations closest to the April 6 mainshock location. The linear best fit is reported as continuous line, the dashed line is the 95% prediction limit.

**Figure 6.** Vp/Vs values calculated for two different time intervals along the AQU-FIAM and AQU-FAGN paths, which are shown in the top panel along with faults (red segments) from Fig. 2.

**Figure 7.** (a) *r–t* plot for the March 30 2009- foreshock relocated events. (b) *r–t* plot for the April 6 2009-April 30 2009 aftershocks relocated events. The spatio-temporal seismicity pattern shows vertically clustered events interrupted by time intervals of seismic quiescence or lowering in the seismic rate. The minimum $M_L$ is 1.0. In both (a) and (b) the symbols are scaled with magnitude $M_L$.

**Figure 8.** Results of the fault slip analysis. Areas with $0 \leq T \leq Ts$ ($Ts$ =1) are the theoretically predicted patterns of poles to reactivated fault planes for different values of $\sigma_1$. Poles to the L'Aquila 2009 reactivated structures A, B, and C are also reported as dots.

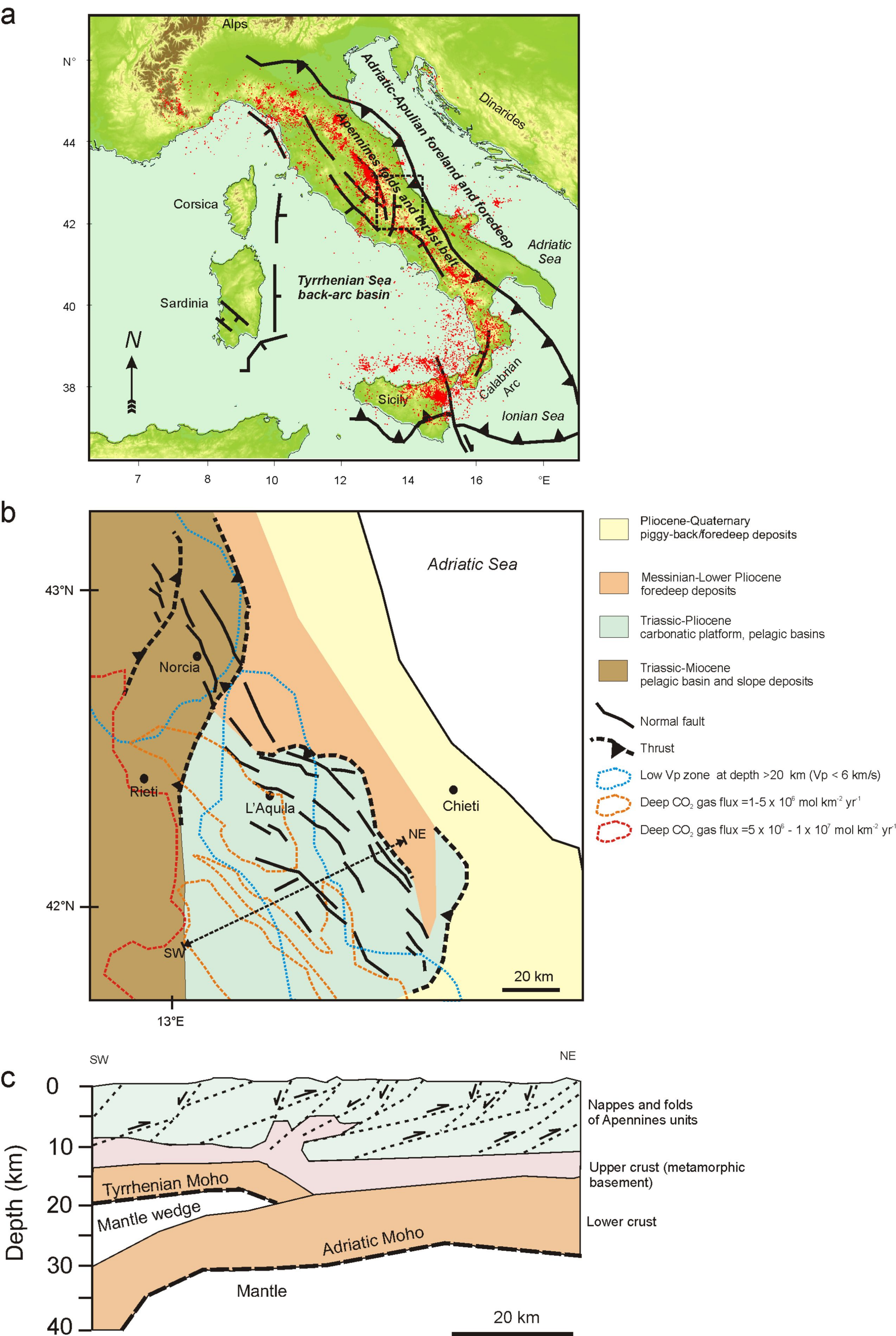
a
Alps
N°
44
42
40
38
7
8
10
12
14
16
°E
Dinarides
Adriatic-Apulian foreland and foredeep
Apennines folds and thrust belt
Corsica
Sardinia
Tyrrhenian Sea
back-arc basin
Adriatic
Sea
Calabrian
Arc
Sicily
Ionian Sea
N
b
Adriatic Sea
43°N
42°N
13°E
Norcia
Rieti
L'Aquila
Chieti
NE
SW
20 km
Pliocene-Quaternary
piggy-back/foredeep deposits
Messinian-Lower Pliocene
foredeep deposits
Triassic-Pliocene
carbonatic platform, pelagic basins
Triassic-Miocene
pelagic basin and slope deposits
Normal fault
Thrust
Low Vp zone at depth >20 km (Vp < 6 km/s)
Deep $CO_2$ gas flux =1-5 x $10^6$ mol $km^{-2}$ $yr^{-1}$
Deep $CO_2$ gas flux =5 x $10^6$ - 1 x $10^7$ mol $km^{-2}$ $yr^{-1}$
c
SW
NE
0
10
20
30
40
Depth (km)
Nappes and folds
of Apennines units
Upper crust (metamorphic
basement)
Lower crust
Tyrrhenian Moho
Mantle wedge
Adriatic Moho
Mantle
20 km

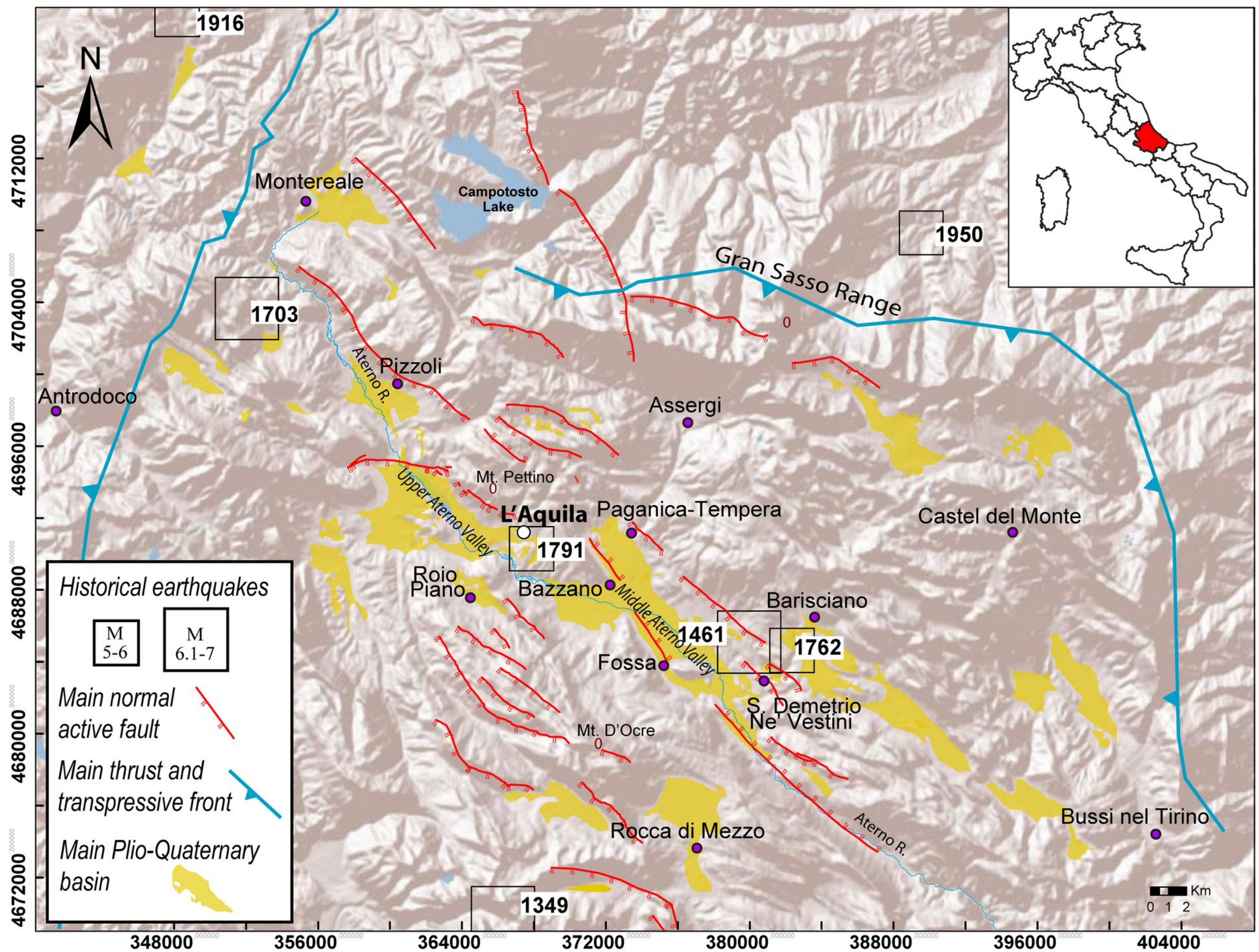
1916
N
Campotosto Lake
Montereale
1950
Gran Sasso Range
1703
Aterno R.
Pizzoli
Antrodoco
Assergi
Mt. Pettino
Upper Aterno Valley
L'Aquila
Paganica-Tempera
Castel del Monte
1791
Roio Piano
Bazzano
Middle Aterno Valley
Barisciano
1461
1762
Fossa
S. Demetrio Ne' Vestini
Mt. D'Ocre
Rocca di Mezzo
Aterno R.
Bussi nel Tirino
1349
Km
0 1 2
Historical earthquakes
M 5-6
M 6.1-7
Main normal active fault
Main thrust and transpressive front
Main Plio-Quaternary basin
4712000
4704000
4696000
4688000
4680000
4672000
348000
356000
364000
372000
380000
388000
396000
404000

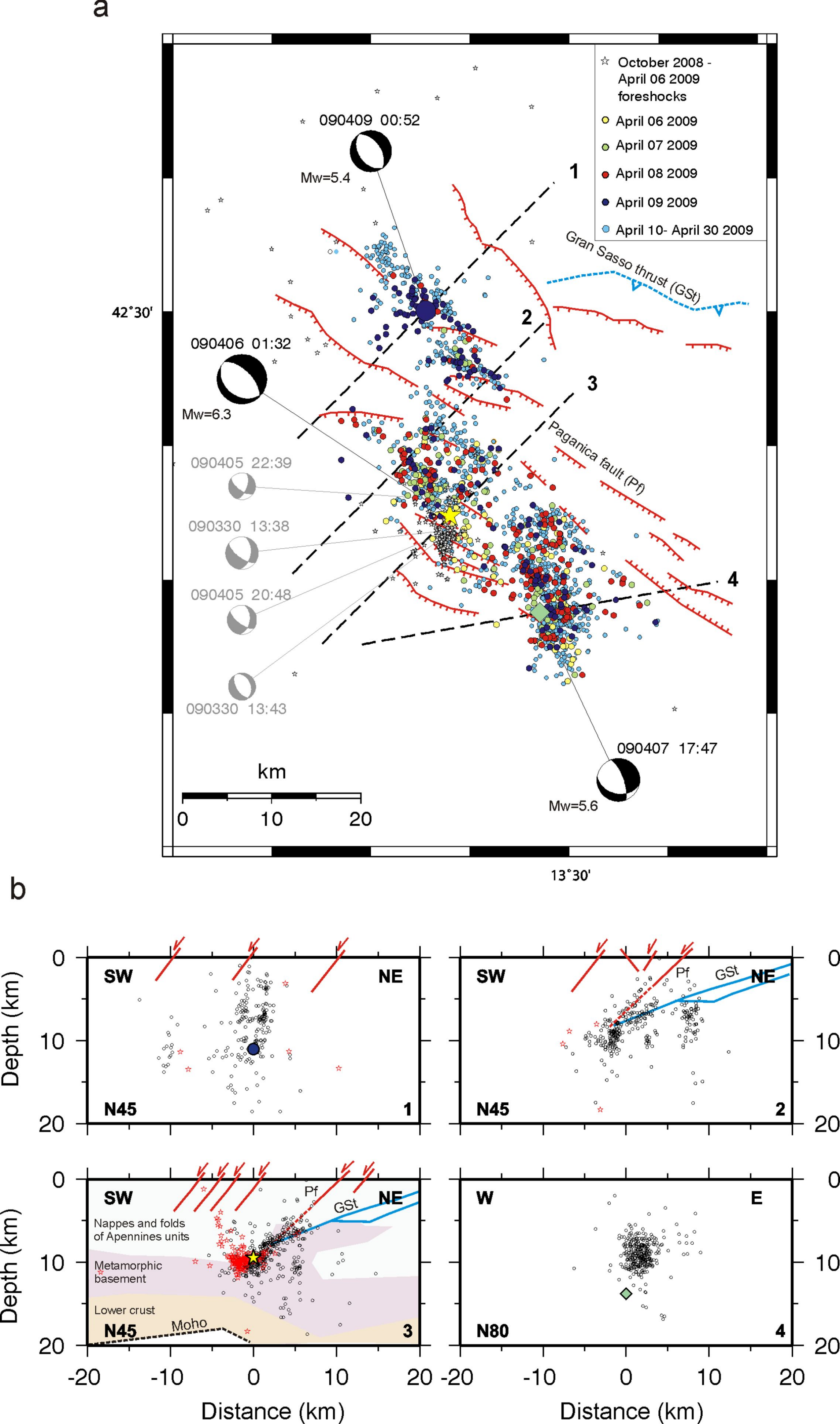

a
October 2008 - April 06 2009 foreshocks
April 06 2009
April 07 2009
April 08 2009
April 09 2009
April 10- April 30 2009
090409 00:52
Mw=5.4
090406 01:32
Mw=6.3
090405 22:39
090330 13:38
090405 20:48
090330 13:43
090407 17:47
Mw=5.6
Gran Sasso thrust (GSt)
Paganica fault (Pf)
1
2
3
4
42°30'
13°30'
km
0
10
20
b
Depth (km)
Distance (km)
SW
NE
N45
W
E
N80
Pf
GSt
Nappes and folds of Apennines units
Metamorphic basement
Lower crust
Moho

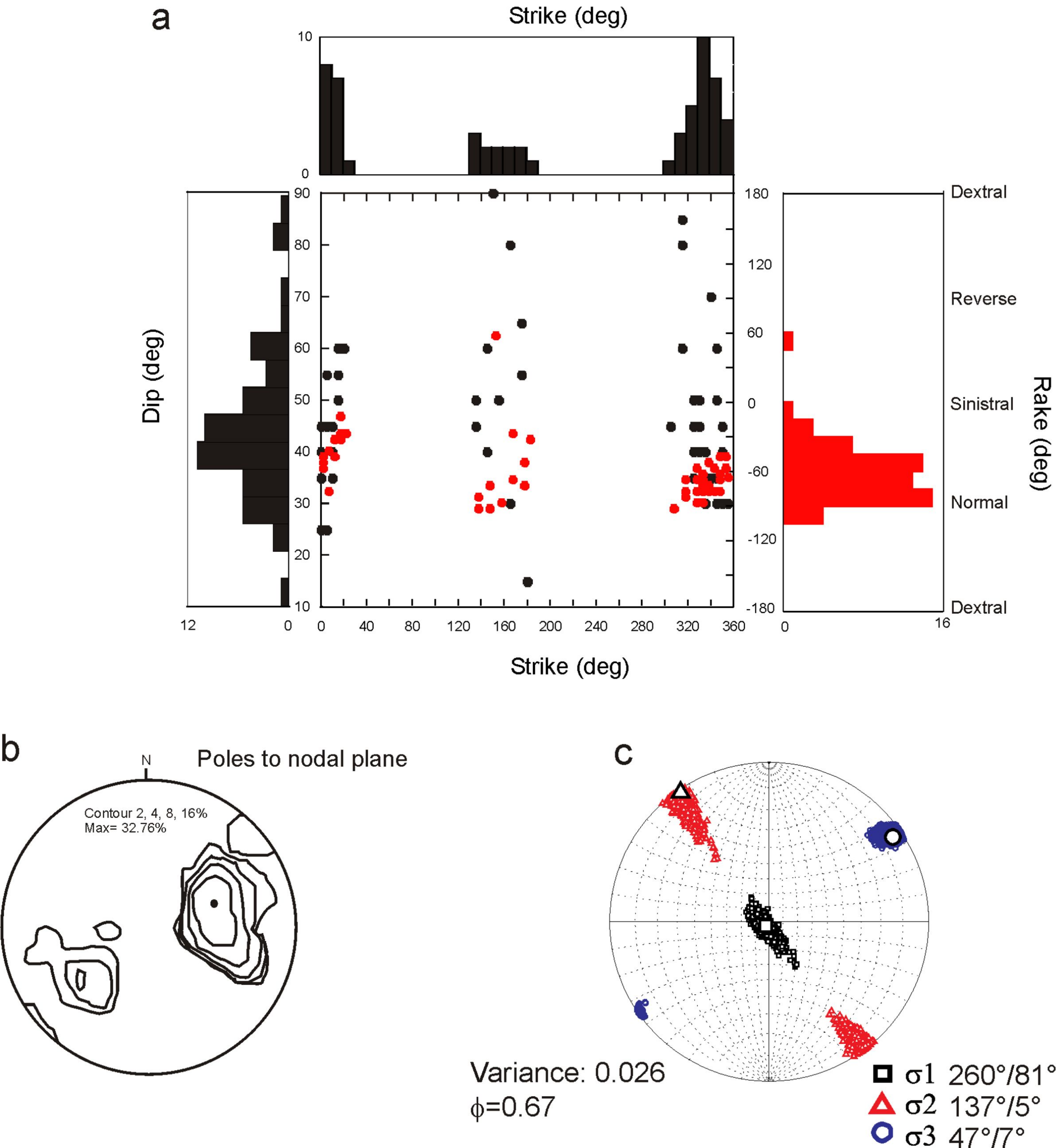
a
Strike (deg)
Dip (deg)
Rake (deg)
Dextral
Reverse
Sinistral
Normal
Dextral
b
N
Poles to nodal plane
Contour 2, 4, 8, 16%
Max= 32.76%
c
Variance: 0.026
ϕ=0.67
σ1 260°/81°
σ2 137°/5°
σ3 47°/7°

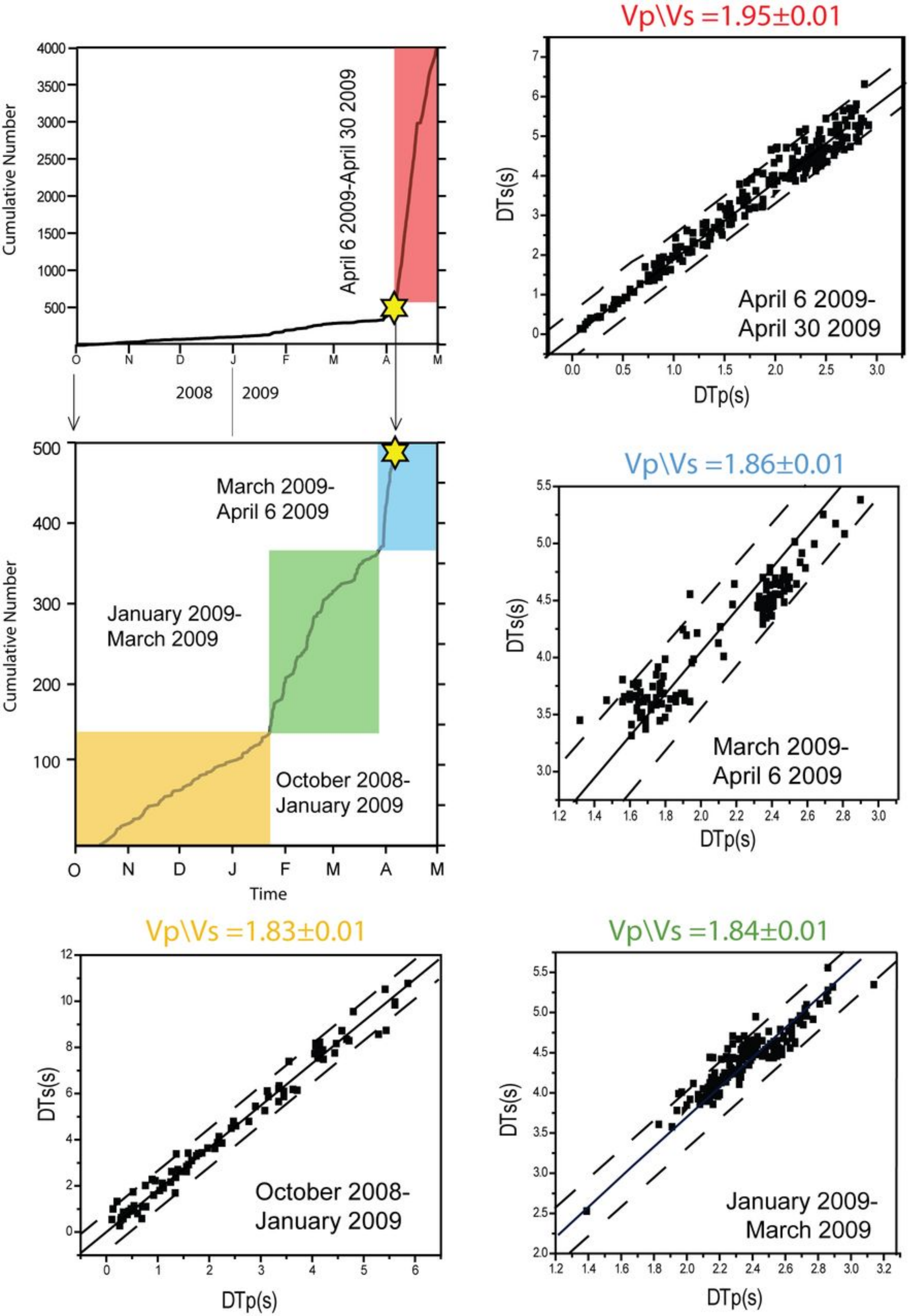

Cumulative Number
April 6 2009-April 30 2009
O N D J F M A M
2008 2009
Vp\Vs =1.95±0.01
DTs(s)
DTp(s)
April 6 2009-
April 30 2009
March 2009-
April 6 2009
January 2009-
March 2009
October 2008-
January 2009
Time
Vp\Vs =1.86±0.01
Vp\Vs =1.83±0.01
Vp\Vs =1.84±0.01

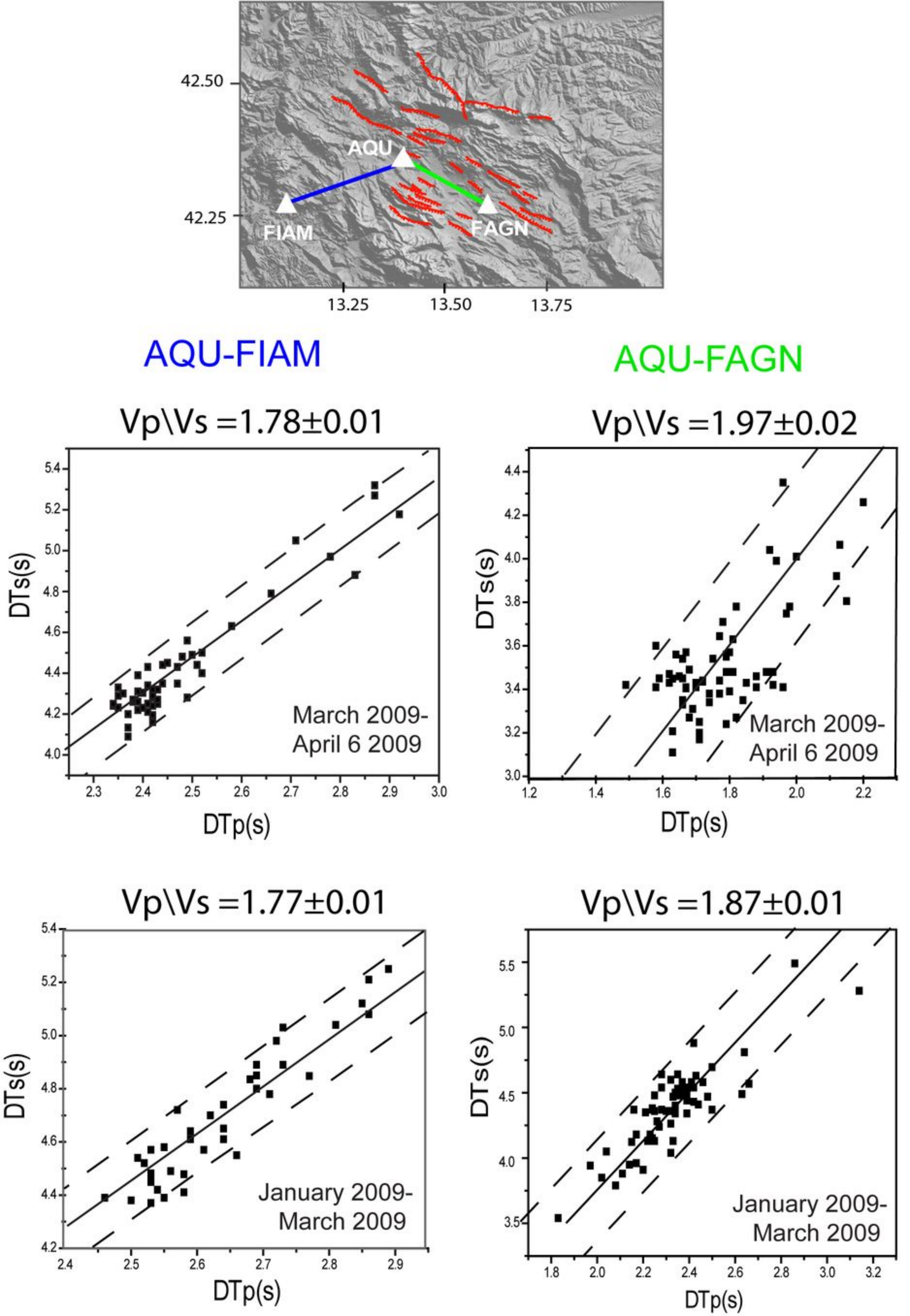
42.50
42.25
AQU
FIAM
FAGN
13.25
13.50
13.75
AQU-FIAM
AQU-FAGN
Vp\Vs =1.78±0.01
Vp\Vs =1.97±0.02
DTs(s)
DTp(s)
March 2009-
April 6 2009
March 2009-
April 6 2009
Vp\Vs =1.77±0.01
Vp\Vs =1.87±0.01
January 2009-
March 2009
January 2009-
March 2009

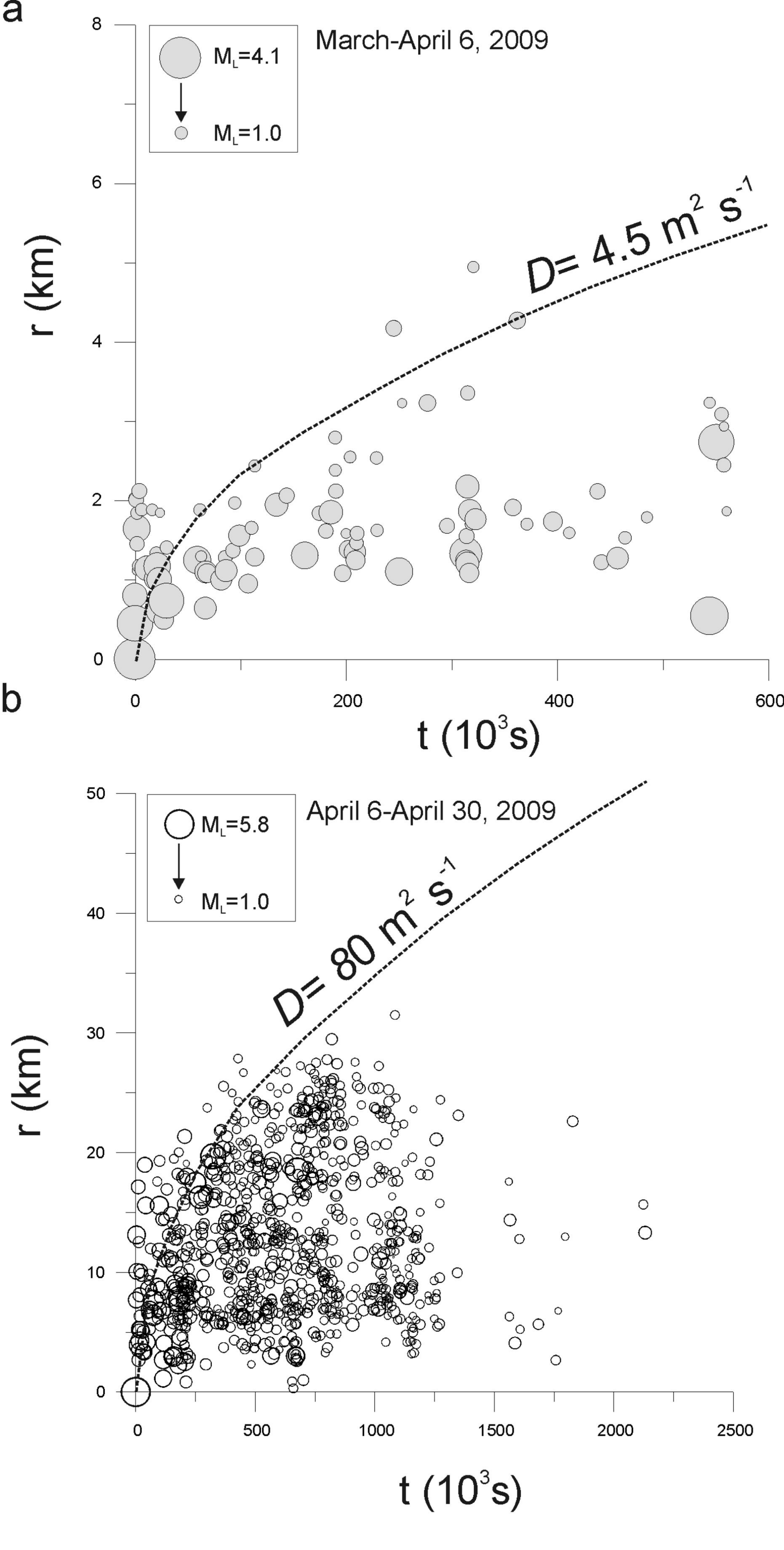
a
March-April 6, 2009
M_L=4.1
M_L=1.0
D= 4.5 m^2 s^-1
r (km)
t (10^3s)
0
2
4
6
8
0
200
400
600
b
April 6-April 30, 2009
M_L=5.8
M_L=1.0
D= 80 m^2 s^-1
r (km)
t (10^3s)
0
10
20
30
40
50
0
500
1000
1500
2000
2500

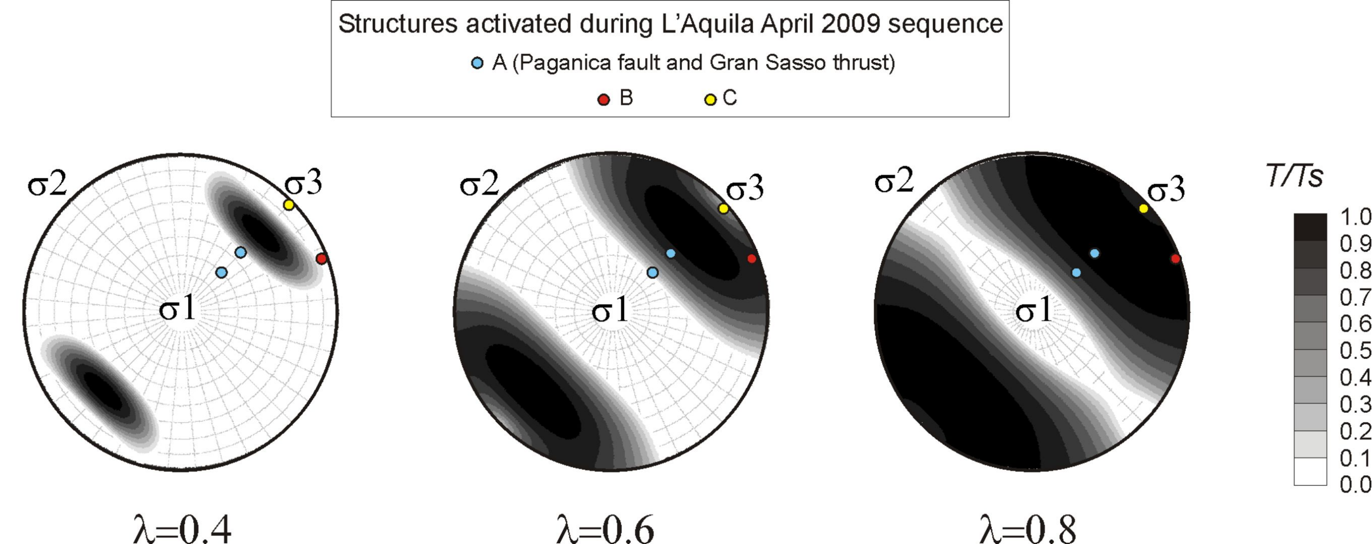
Structures activated during L'Aquila April 2009 sequence
A (Paganica fault and Gran Sasso thrust)
B
C
σ2
σ3
σ1
σ2
σ3
σ1
σ2
σ3
σ1
T/Ts
1.0
0.9
0.8
0.7
0.6
0.5
0.4
0.3
0.2
0.1
0.0
λ=0.4
λ=0.6
λ=0.8